The Unusual Solid-State Structure of Mercury Oxide: Relativistic Density Functional Calculations for the Group 12 Oxides ZnO, CdO, and HgO†

Susan Biering,‡ Andreas Hermann,‡ Jürgen Furthmüller,§ and P. Schwerdtfeger*,‡

Centre for Theoretical Chemistry and Physics, The New Zealand Institute for Advanced Study, Massey University Albany, Private Bag 102904, North Shore City, 0745 Auckland, New Zealand, and Institut für Festkörpertheorie und -optik, Friedrich-Schiller-Universität Jena, Max-Wien-Platz 1, D-07743 Jena, Germany

Received: March 22, 2009; Revised Manuscript Received: April 15, 2009

The solid-state structure of mercury oxide and its low-pressure modifications are known to significantly differ from those found for the corresponding zinc and cadmium compounds, that is, one changes from a simple hexagonal wurtzite or cubic rock salt structure found in zinc oxide and cadmium oxide to unusual chainlike montroydite and cinnabar structures in mercury oxide. Here, we present relativistic and nonrelativistic density functional studies which demonstrate that this marked structural difference is caused by relativistic effects. For HgO, the simple rock salt structure is only accessible at higher pressures. Relativistic effects reduce the cohesive energy by 2.2 eV per HgO unit and decrease the density of the crystal by 14% due to a change in the crystal symmetry. Band structure and density of states calculations also reveal large changes in the electronic structure due to relativistic effects, and we argue that the unusual yellow to red color of HgO is a relativistic effect as well.

Introduction

Mercury oxide, HgO, is a solid that, unlike its lighter congeners, decomposes quite easily into mercury and oxygen, as first observed in a famous experiment by Joseph Priestley and reported in 1775.[1] This implies that the mercury−oxygen bond in free HgO is rather weak (dissociation energy of only 0.17 eV, according to a recent analysis of Shepler and Peterson),[2] which was the subject of a recent debate.[2,3] More recent critical discussions can be found in the articles of Filatov and Cremer[4] and Peterson et al.[5]

Solid HgO is rather unusual as well, as it crystallizes in an orthorhombic *Pnma* structure, where planar O−Hg−O zigzag chains are formed parallel to the *a* axis in the *ac* plane (see Figure 1), and in a cinnabar phase with spiral-like chains.[6−8] In contrast, the group 12 chalcogenides ZnO and CdO are known to crystallize in simple cubic or hexagonal structures at room temperature and low pressures. Only at high pressures does HgO undergo a phase transition to the tetragonal phase (*I*4/*mmm*),[9] and at even higher pressures, a metallic phase was identified with a rock salt structure.[10] We mention that HgO is used as the anode material in mercury batteries or in the synthesis of high-temperature mercury-based superconductors,[11] to name but a few applications.

Understanding the role of structure for bulk properties is an important aspect in the design of new materials. However, it is currently hard (if not impossible) to predict solid-state structures from simple bonding models[12] (see also the response by Cohen),[13] especially if polymorphs are separated only by small energies. The unusual low-pressure modifications of HgO, the montroydite and cinnabar structures, are prime examples of this dilemma that we face in solid-state chemistry or physics. This is in stark contrast to molecular structures, where simple bonding models are very successful. Here, we show that the two low-pressure montroydite and cinnabar modifications of HgO, only found in mercury compounds, are a result of relativistic effects.

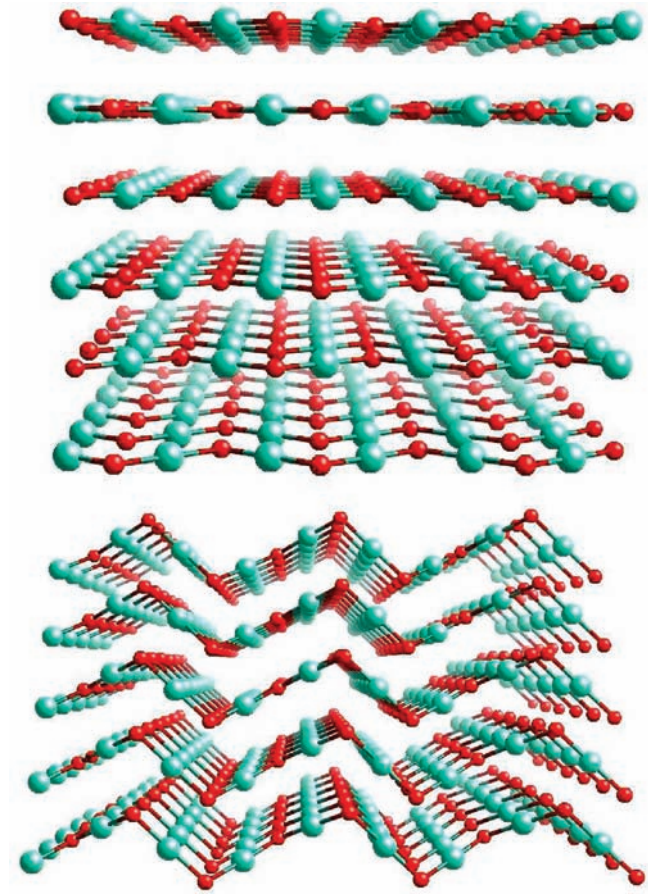

Figure 1. The montroydite (top) and cinnabar crystal structure of HgO (bottom).

† Part of the "Russell M. Pitzer Festschrift".

* To whom correspondence should be addressed. E-mail: p.a.schwerdtfeger@massey.ac.nz.

‡ Massey University Albany.

§ Friedrich-Schiller-Universität Jena.

10.1021/jp9025915 CCC: $40.75
Published on Web 04/30/2009

Relativistic effects are well-known to play an important role in molecular structures of mercury-containing compounds[14−22] but have not been investigated yet in detail for the solid state.[23,24]

Computational Method

All calculations were carried out using density functional theory within a periodic boundary framework, employing a plane wave basis as implemented in the Vienna ab initio simulation package VASP.[25] The electron−electron interaction was treated within the generalized gradient approach (GGA)[26] for the exchange−correlation energy, using the parametrization by Perdew and Wang (PW91).[27] The atomic core region was described by means of the projector-augmented wave (PAW) method[28,29] with the outermost $(n - 1)$dns electrons in the valence space. Relativistic effects were included within the frozen core approximation for all elements considered. Nonrelativistic calculations were carried out only for HgO, as relativistic effects are much smaller in the case of ZnO and CdO, and therefore, nonrelativistic results for these two solid state systems were expected to resemble those of the relativistic ones. The plane wave expansion of the wave functions in the present case was carefully checked for convergence and, in general, restricted to a maximum kinetic energy of 33 Ry, except for the relativistic HgO montroydite structure where a 43 Ry cutoff was necessary. Integrations over the Brillouin zone were carried out by summing over a uniform k-point mesh including the Gamma point, where the number of k-points was chosen to obtain a converged total energy. Meshes of $5 \times 5 \times 5$ (CdO and relativistic HgO in rock salt and zinc blende structure), $6 \times 6 \times 6$ (ZnO and nonrelativistic HgO in rock salt and zinc blende structure, CdO and non/relativistic HgO in cesium chloride structure), $5 \times 5 \times 2$ (CdO and relativistic HgO in wurtzite structure), $6 \times 6 \times 2$ (ZnO and nonrelativistic HgO in wurtzite structure), $3 \times 3 \times 2$ (relativistic HgO in cinnabar structure), $2 \times 2 \times 3$ (relativistic HgO in montroydite structure), $6 \times 6 \times 3$ (nonrelativistic HgO in cinnabar structure), and $3 \times 3 \times 6$ (nonrelativistic HgO in montroydite structure) proved to be sufficient.

To obtain the equilibrium crystal properties, a full geometry optimization was carried out for the different crystal structures of ZnO, CdO, and HgO, that is, the cell shape as well as the internal Wyckoff parameters of the respective structures' unit cells were optimized over a range of fixed unit cell volumes. The energy−volume relationships were used to obtain the lattice parameters, as well as the bulk moduli, by fitting them to the Murnaghan equation of state (EOS).[30] From this, one obtains directly the pressure as $p = -\mathrm{d}E/\mathrm{d}V$, the equilibrium volume V_0, the total energy per cation−anion pair E_0, the bulk modulus B, and the pressure coefficient $B' = \mathrm{d}B/\mathrm{d}p$. From the total energy per cation−anion pair, the cohesive energy (atomization energy) was determined by subtracting the atomic total energies. The latter were obtained through single atom calculations for Zn, Cd, Hg, and O in a box of well-defined size using a plane wave cutoff equivalent to the one used in the crystal calculations. Spin polarization was included in the case of oxygen. The transition pressure was estimated for the low-temperature limit only, that is, instead of the Gibbs free energy $G = U + pV - TS$ defining the crystal stability for a given temperature and pressure, we use the enthalpy $H = E + pV$, where $U(V) \approx E(V)$. We neglect the zero-point energy. From the enthalpy versus pressure plot, we obtain the transition pressure as the crossing of two curves of different crystal structures.

For the electronic properties of the various crystal structures, the corresponding band structures are computed directly by solving the Kohn−Sham equations.[31] Even though this implies an underestimation of the fundamental band gap and interband excitation energies due to the density functional chosen within the single-particle picture applied,[32,33] this method usually leads to reasonable qualitative results for the dispersion and orbital character of the valence and conduction bands. The path for the calculations was chosen according to the Bilbao crystallographic server.[34,35] To calculate the electronic density of states (DOS), we integrated over the Brillouin zone using the tetrahedron method[36] with increased k-point meshes of $35 \times 35 \times 35$ for the HgO rock salt structure in the nonrelativistic case, $15 \times 15 \times 23$ for the montroydite phase scalar relativistic calculations, and $5 \times 6 \times 9$ for the more computer time expensive spin−orbit coupled calculations.

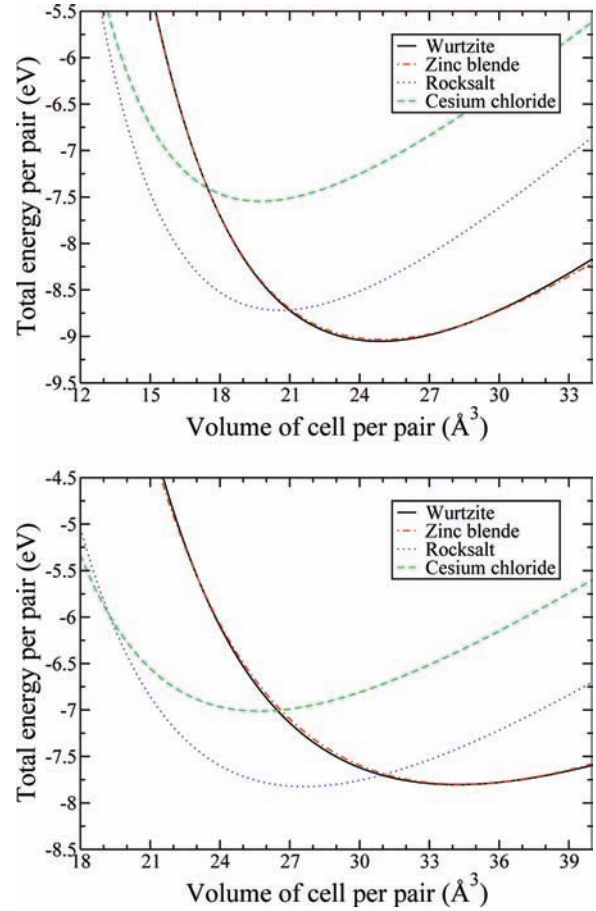

Figure 2. Lattice energies for different crystal structures of ZnO (top) and CdO (bottom).

Results and Discussion

Figure 2 shows the energy−volume curves for different crystal structures of ZnO, which confirms the fact that it crystallizes in a wurtzite structure under normal conditions. The calculated lattice parameters of $a = 3.279$ Å, $c = 5.304$ Å, and (internal Wyckoff position) $z_O = 0.3785$[37] and other properties (cf. Table 1) compare very well to experimental results ($a = 3.258$ Å, $c = 5.220$ Å, and $z_O = 0.382$)[38] and previously published theoretical work ($a = 3.283$ Å, $c = 5.309$ Å, and $z_O = 0.3786$).[39] The deviations in the bulk modulus are recorded in other theoretical investigations as well[39] and are most likely a finite temperature effect. For the zinc blende structure of ZnO, we obtain a lattice constant of $a = 4.622$ Å and a cohesive energy of $E_{coh} = 7.28$ eV. Hence, this crystal arrangement is very close to the wurtzite structure.[39]

TABLE 1: Ground-State Properties of Equilibrium and High-Pressure Phases with Closest Metal−Oxygen Bond Distances d_{MO} and Closest Metal−Metal Distances d_{MM} in Å, Bulk Moduli B in GPa and Their Derivatives $B' = dB/dp$, Cohesive Energies E_{coh} in eV, and the Volume V_0 in Å^3

system	d_{MO}	d_{MM}	B	B'	E_{coh}	V_0
			ZnO			
wurtzite	2.000	3.258	131.1	4.4	7.29	24.70
exp[38,40]	1.977	3.207	181	4	7.52	23.99
zinc blende	2.001	3.268	130.9	4.6	7.28	24.68
rock salt	2.167	3.065	168.5	5.5	6.99	20.35
exp[41]	2.136	3.020	228	4		19.48
cesium chloride	2.330	2.690	161.9	4.6	5.83	19.46
			CdO			
rock salt	2.389	3.379	130.1	4.0	6.08	27.29
exp[40,42]	2.348	3.321	148	4	6.40	25.89
wurtzite	2.226	3.613	91.9	4.2	6.06	34.11
zinc blende	2.229	3.640	94.3	4.4	6.04	34.13
cesium chloride	2.544	2.938	130.5	4.4	5.28	25.37
exp[43]	2.48	2.86	169	4.66		23.39
			HgO			
montroidyte	2.064	3.375	20.7	9.7	4.04	36.04
exp[6,9]	2.028	3.306	44	7		32.13
cinnabar	2.065	3.331	20.5	5.9	4.03	36.39
exp[8]	2.03	3.30				32.07
zinc blende	2.299	3.754	82.1	5.5	3.83	37.41
exp[44]	2.35	3.84				40.03
tetragonal	2.427	3.475	110.6	5.9	3.75	30.02
exp[9]	2.33	3.33	44	7		32.15
rock salt	2.469	3.491	112.3	3.8	3.74	30.08
cesium chloride	2.622	3.028	120.8	5.3	3.09	27.77
			HgO (nonrel.)			
rock salt	2.498	3.533	113.6	5.5	6.20	31.17
wurtzite	2.333	3.851	79.4	3.5	6.06	39.28
zinc blende	2.338	3.818	81.5	5.4	6.03	39.36
cesium chloride	2.655	3.066	117.4	4.8	5.48	28.83

Under ambient conditions, CdO crystallizes in the rock salt structure. This again is confirmed by our calculations; see Figure 2. As for the lattice parameters, we obtain $a = 4.779$ Å, in good agreement with the experimental value ($a = 4.696$ Å[42]). Other theoretical calculations yield similar results ($a = 4.779$ Å[39]). The energy−volume dependencies were also calculated for the wurtzite phase ($a = 3.669$ Å, $c = 5.852$ Å, $z_O = 0.3833$, and values listed in Table 1) and for the zinc blende structure ($a = 5.149$ Å). Again, the cohesive energies of these two phases are fairly similar; see Table 1 and ref 39.

Turning now to HgO, the orthorhombic form known as montroydite has lattice parameters of $a = 6.612$ Å, $b = 5.520$ Å, and $c = 3.521$ Å, Wyckoff positions $x_{Hg} = 0.112$, $z_{Hg} = 0.243$, $x_O = 0.358$, and $z_O = 0.587$,[6] and the energetically close-lying HgS-like cinnabar form with $a = 3.577$ Å, $c = 8.681$ Å, $x_{Hg} = 0.745$, and $x_O = 0.460$.[8,37] In our calculations, we obtain lattice constants of $a = 6.747$ Å, $b = 5.779$ Å, and $c = 3.697$ Å, with $x_{Hg} = 0.112$, $z_{Hg} = 0.243$, $x_O = 0.360$, and $z_O = 0.571$ as parameters for the orthorhombic structure. This compares very well to other theoretical calculations ($a = 6.74$ Å, $b = 5.68$ Å, $c = 3.68$ Å).[45] For the cinnabar phase, we obtain $a = 3.745$ Å, $c = 8.968$ Å, $x_{Hg} = 0.745$, and $x_O = 0.414$, all in reasonable agreement with the experimental results. These deviations are acceptable considering the very shallow potential curve (see Figure 3) expressed by the very small bulk moduli, Table 1. Nevertheless, we accurately predict these two crystal structures as low-pressure modifications. In the case of the high-pressure zinc blende structure for HgO, proposed as a metastable sphalerite phase in shock-compression experiments on HgO by Ovsyannikova et al.,[44] the calculated bond distances are overestimated. This is most likely due to the difficulties in examining metastable phases in general or to the density functional approximation used.

If we neglect relativistic effects, we find a completely different picture; see Figure 3. In that case, the low-pressure phase is the rock salt structure with a lattice constant of $a = 4.996$ Å, larger than that of ZnO and CdO. Also, the nonrelativistic cohesive energy of 6.20 eV is more than 2 eV larger than the relativistic value. Interestingly, this rather large relativistic lattice destabilization goes along with a huge relativistic contraction of 0.434 Å in the intrachain Hg−O distances, Table 1. Thus, the bond distance in HgO is as small as the ZnO bond distance for the wurtzite structure. However, this intrachain contraction induces an interchain expansion in the b direction with an interchain Hg−O distance of 2.964 Å, resulting in an overall volume expansion from 31.2 to 36.0 Å^3 due to the change in crystal symmetry and a consequent decrease in density from 11.54 to 9.98 g cm^{-3} (exp. 11.14 g cm^{-3})[40] upon inclusion of relativistic effects (compare to ZnO with 5.6 g cm^{-3} or CdO with 8.15 g cm^{-3}).[40] Even more interesting is that at the nonrelativistic level, both the montroydite and the cinnabar phases relax into the rock salt structure upon relaxation. Hence, both the cinnabar and montroydite phase are kinetically unstable at the nonrelativistic level, and the existence of these two phases can be credited to relativistic effects.

Relativistic effects are well-known in molecules containing heavy elements,[14,46] but little attention has been given so far to their influence on solid-state properties[47−51] and resulting changes in crystal symmetry.[24,52] Only one recent investigation has shown that changes in crystal symmetry of group 11 monohalides are due to relativistic effects[52,53] (see also more recent work on AuF by Kurzydłowski and Grochala, which

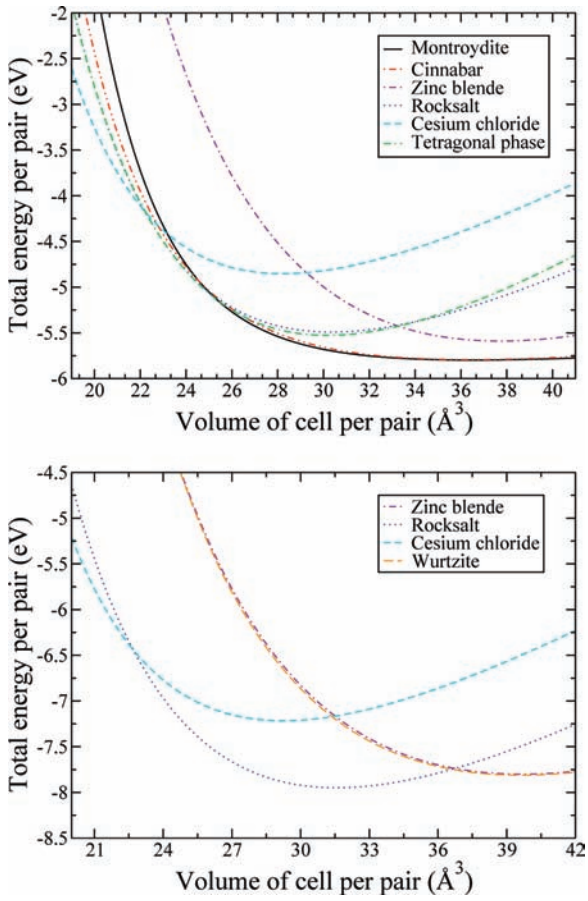

Figure 3. Relativistic (top) and nonrelativistic (bottom) lattice energies for different crystal structures of HgO.

includes a discussion of high-pressure modifications).[54,55] Here, we have a similar situation. Diatomic HgO is relativistically destabilized (dissociation energy at the nonrelativistic level is 1.0 eV compared to only 0.17 eV at the relativistic level[2]), which explains that HgO easily decomposes in the gas phase. Our calculations reveal that the HgO dipole moment is significantly reduced due to relativistic effects, that is, from 8.0 to 5.7 D (at the Hartree−Fock level treating the electron correlation by second-order many-body perturbation theory). Hence, HgO becomes less ionic due to relativistic effects, and covalent bonding in the solid state is substantially increased. Indeed, the Mulliken charge for the mercury atom in solid HgO decreases from +1.10 at the nonrelativistic level (rock salt phase) to +0.90 at the relativistic level (montroydite phase). Hence, typical ionic structures like the rock salt structure become less favorable. Note also the large relativistic destabilization of solid HgO, that is, the cohesive energy drops from 6.2 to 4.0 eV per HgO unit upon inclusion of relativity, substantially more than that for the molecule.[2] As spin−orbit coupling is suppressed in the ionic lattice field, we assume that the structural change originates almost exclusively from scalar relativistic (mass−velocity) effects, but spin−orbit effects are important to determine the exact band gap in HgO (see discussion below). Note that the sublimation energies of group 12 chalcogenides have recently been discussed in detail by Szentpály.[56]

The ZnO crystal structure undergoes a phase transition from the hexagonal wurtzite structure to the cubic rock salt structure with increasing pressure (see Figure 2). We calculate a transition pressure to the high-pressure rock salt phase of 13 GPa (lattice constant $a = 4.334$ Å), in reasonable agreement with experiment (9.1 GPa,[57] $a = 4.271$ Å[41]); see also recent theoretical work.[39,58] Furthermore, a transition to the cesium chloride structure ($a = 2.690$ Å) occurs at 261 GPa, which has not been confirmed yet experimentally considering the very high pressure but was also predicted in refs 39 and 59. The picture for CdO is slightly different. Here, the equilibrium phase is the rock salt structure. The transition to the cesium chloride structure occurs at 84 GPa with a lattice constant of $a = 2.938$ Å, in accordance with experimental work (90 GPa)[43] and previous theoretical calculations.[39,60]

Concerning the high-pressure phases of HgO, we obtain a transition into a tetragonal phase with space group *I*4/*mmm* at approximately 25 GPa. This phase is a distortion of the rock salt structure, where *c*/*a* differs only slightly from the optimum of $\sqrt{2} = 1.414$. With our calculated values of $a = 3.517$ Å and $c = 4.854$ Å, we obtain $c/a = 1.380$, in good agreement with experiment ($a = 3.370$ Å, $c = 4.651$ Å, $c/a = 1.380$, $P = 14$ GPa[9]). A further transition to the metallic state, which is identified as the rock salt structure, occurs at 26 GPa.[10] We obtain this transition at a pressure of approximately 28 GPa with $a = 4.937$ Å, although this transition pressure is hard to predict since the enthalpy versus pressure curves of those two structures are almost parallel in this region. In addition, we predict another transition at around 57 GPa into the cesium chloride structure ($a = 3.028$ Å). In the nonrelativistic case, a phase transition from the common rock salt structure to the cesium chloride structure occurs at 62 GPa ($a = 3.066$ Å). Furthermore, the tetragonal phase (*I*4/*mmm*) is not stable anywhere in the nonrelativistic regime studied here. Hence, the nonrelativistic structural transition path of HgO closely resembles that of CdO.

We also investigated the influence of relativistic effects on the electronic structure of HgO and obtained the band structure and density of states (DOS) for the ground state of the equilibrium phase of HgO at the relativistic as well as nonrelativistic level of theory including also spin−orbit coupling. HgO in its ground state is reported to be an n-type II−VI semiconductor[9] with a band gap of approximately 2.19[61] to 2.80 eV[62] through photoconductivity measurements. Theoretical investigations reported in ref 9 confirm this result using a scalar relativistic tight-binding linear muffin-tin orbital atomic sphere approximation but also show that for DFT methods commonly applied, the band gap is underestimated as they yield an indirect gap of 1.33 eV. In the scalar relativistic approach, our results predict HgO to be an indirect semiconductor as well; see Figure 4. The valence band maximum (VBM) occurs at the H line between T and Y, and the conduction band minimum (CBM) is at the Λ line between Γ and Z, leading to a fundamental gap of 1.18 eV. Several other indirect as well as direct transitions are possible at slightly higher energies, the first possible direct transition at the Δ line between Y and Γ at an energy of 1.49 eV. This is in agreement with the theoretical findings mentioned above but neglects spin−orbit coupling. We expect that the relativistic expansion of the $5d_{5/2}$ band in mercury will lead to a substantial mixing with the 6s band, and one has to consider the spin−orbit splitting in the empty 6p bands as well. Comparing this to the band structure and DOS calculated with the inclusion of spin−orbit coupling (Figure 4), a dramatical difference can be found. In this case, montroydite needs to be characterized as a metal. This clearly false description of GGA, that is, the severe underestimation of the gand gap, is well-known in Mott insulators in transition-metal oxides[63] or for the δ-phase of solid plutonium[64] and was already discussed in detail in ref 63. This is due to strong correlation effects in these

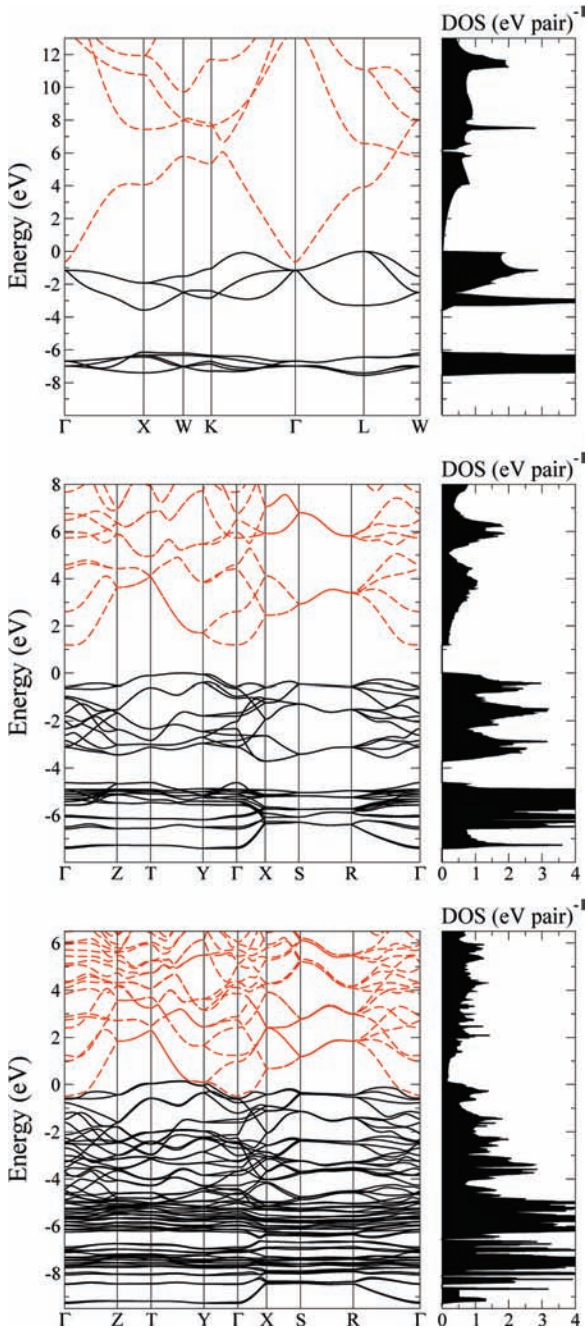

Figure 4. Band structure and density of states for HgO, the nonrelativistic rock salt structure (top), the montroydite scalar relativistic structure (middle), and the relativistic montroydite structure including spin−orbit coupling (bottom). The valence band maximum and the Fermi energy are set to zero energy. The black solid lines indicate the valence and the red dashed lines the conducting bands.

transition-metal oxides making a further investigation using methods like LDA+U desirable.[65]

Turning again to the nonrelativistic equilibrium state of HgO, the rock salt structure, we observe a rather different behavior. The VBM can be found at the Σ line between Γ and K and at the L point, and the CBM occurs at the Γ point, Figure 4. Since the VBM lies above the CBM, we find negative indirect band gaps of −0.56 and −0.64 eV, respectively. This suggests a half metal at the nonrelativistic level, similar to that found for CdO.[39] The smallest direct gap occurs at the Γ point with an energy of 0.52 eV.

Looking at the Hg site-projected nonrelativistic DOS (upper panel of Figure 5), we find a well-defined crystal field splitting

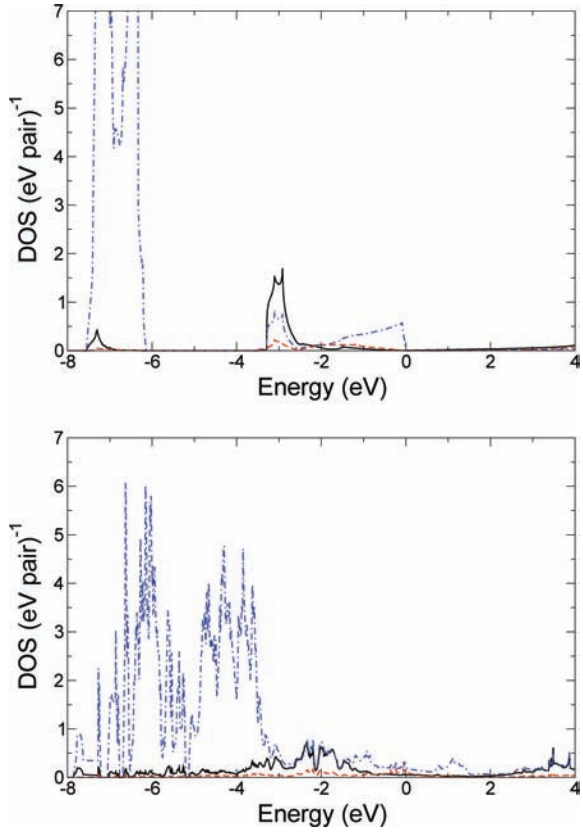

Figure 5. Site-projected density of states for HgO nonrelativistic rock salt (top) and for HgO relativistic montroydite including spin−orbit coupling (bottom). The black solid, red dashed, and blue dash−dotted lines indicate the s, p, and d site-projected DOS, respectively.

for the d bands of approximately 0.8 eV, which is due to the octahedral arrangement in the rock salt structure. In contrast, the Hg site-projected DOS including spin−orbit coupling for the montroydite structure becomes far more complex. Here, the influence of the spin−orbit coupling is prominent in the splitting of the Hg core 5d band into the $5d_{3/2}$ and $5d_{5/2}$ contributions, with an energy difference of about 2 eV that agrees nicely with the atomic-level splitting of 1.86 eV in the Hg^+ atom.[66] Still, the superposition with the crystal field splitting can be seen. This should be investigated further by spectroscopic methods. We mention that the Fermi edge has dominantly O 2p and Hg 5d character.

Conclusion

In summary, we have shown that the low-pressure modifications of solid mercury oxide differ significantly from those found for the corresponding zinc and cadmium compounds as a result of scalar relativistic effects, similar to those observed for the gold halides.[52,53] The loss of ionic nature (increase in covalency) in HgO due to relativistic effects gives rise to the unusual chainlike montroydite and cinnabar structures in mercury oxide. Both scalar and spin−orbit relativistic effects influence the band structure of HgO considerably. In an attempt to estimate the influence of relativistic effects on the color of mercury oxide, we used the fundamental gap as a first indicator. Thereby, the scalar relativistic calculations suggest a direct band gap transition of about 830 nm as compared to the 2400 nm in the nonrelativistic case. Furthermore, spin−orbit effects lead to a closure of the band gap at the level of theory applied. As mentioned earlier, the band gap is severely underestimated in DFT calculations; hence, we cannot make an absolute prediction about

the color of the solids as such. However, from the difference in wavelength, it is most likely that the yellow to red color of HgO is indeed a relativistic effect. To calculate the onset of the optical absorption accurately will, however, remain a challenge to theoretical solid-state physics.

Acknowledgment. We thank the Royal Society of New Zealand (Marsden Grant 07-MAU-016) for financial support and Dr. Tilo Söhnel (Auckland University) and Christian Thierfelder for valuable discussions and help.

References and Notes

(1) Priestley, J. *Philos. Trans.* **1775**, *65*, 384.
(2) Shepler, B. C.; Peterson, K. A. *J. Phys. Chem. A* **2003**, *107*, 1783.
(3) Chase, M. W., Jr.; Davies, C. A.; Downey, J. R., Jr.; Frurip, D. J.; McDonald, R. A.; Syverud, A. N. *J. Phys. Chem. Ref. Data* **1985**, *14*.
(4) Filatov, M.; Cremer, D. *ChemPhysChem* **2004**, *5*, 1547.
(5) Peterson, K. A.; Shepler, B. C.; Singleton, J. M. *Mol. Phys.* **2007**, *105*, 1139.
(6) Voronin, V. A.; Shchennikov, V. V. *Kristallografiya* **1989**, *34*, 491.
(7) Aurivillius, K.; Carlsson, I. B. *Acta Chem. Scand.* **1956**, *10*, 852.
(8) Aurivillius, K.; Carlsson, I. B. *Acta Chem. Scand.* **1958**, *12*, 1297.
(9) Zhou, T.; Schwarz, U.; Hanfland, M.; Liu, Z. X.; Syassen, K.; Cardona, M. *Phys. Rev. B* **1998**, *57*, 153.
(10) Nelmes, R. J.; McMahon, M. I. In *High Pressure Semiconductor Physics I*; Suski, T., Paul, W., Eds.; Academic: New York, 1998; pp 146−247.
(11) Schilling, A.; Cantoni, M.; Guo, J. D.; Ott, H. R. *Nature* **1993**, *363*, 56.
(12) Maddox, J. *Nature* **1988**, *335*, 201.
(13) Cohen, M. L. *Nature* **1989**, *338*, 291.
(14) Pyykkö, P. *Chem. Rev.* **1988**, *88*, 594.
(15) Schwerdtfeger, P. *J. Am. Chem. Soc.* **1990**, *112*, 2818.
(16) Norrby, L. J. *J. Chem. Educ.* **1991**, *68*, 110.
(17) Schwerdtfeger, P.; Boyd, P. D. W.; Brienne, S.; McFeaters, J. S.; Dolg, M.; Liao, M. S.; Schwarz, W. H. E. *Inorg. Chim. Acta* **1993**, *213*, 233.
(18) Schwerdtfeger, P.; Li, J.; Pyykkö, P. *Theoret. Chim. Acta* **1994**, *87*, 313.
(19) Nakatsuji, H.; Hada, M.; Kaneko, H.; Ballard, C. C. *Chem. Phys. Lett.* **1996**, *255*, 195.
(20) Wesendrup, R.; Laerdahl, J. K.; Schwerdtfeger, P. *J. Chem. Phys.* **1999**, *110*, 9457.
(21) Schwerdtfeger, P.; Wesendrup, R.; Moyano, G. E.; Sadlej, A. J.; Greif, J.; Hensel, F. *J. Chem. Phys.* **2001**, *115*, 7401.
(22) Wang, X.; Andrews, L.; Riedel, S.; Kaupp, M. *Angew. Chem., Int. Ed.* **2007**, *119*, 8523.
(23) Singh, P. P. *Phys. Rev. B* **1994**, *49*, 4954.
(24) Gaston, N.; Paulus, B.; Rosciszewski, K.; Schwerdtfeger, P.; Stoll, H. *Phys. Rev. B* **2006**, *74*, 094102.
(25) Kresse, G.; Furthmüller, J. *Comput. Mater. Sci.* **1996**, *6*, 15.
(26) Perdew, J. P.; Chevary, J. A.; Vosko, S. H.; Jackson, K. A.; Pederson, M. R.; Singh, D. J.; Fiolhais, C. *Phys. Rev. B* **1992**, *46*, 6671.
(27) Perdew, J. P. In *Electronic Structure of Solids*; Ziesche, P., Eschrig, H., Eds.; Akademie Verlag: Berlin, Germany, 1991.
(28) Blöchl, P. E. *Phys. Rev. B* **1994**, *50*, 17953.
(29) Kresse, G.; Joubert, D. *Phys. Rev. B* **1999**, *59*, 1758.
(30) Murnaghan, F. D. *Proc. Natl. Acad. Sci. U.S.A.* **1944**, *30*, 244.
(31) Kohn, W.; Sham, L. J. *Phys. Rev.* **1965**, *140*, A1133.
(32) Hybertsen, M. S.; Louie, S. G. *Phys. Rev. B* **1986**, *34*, 5390.
(33) Bechstedt, F. *Adv. Solid State Phys.* **1992**, *32*, 161.
(34) Aroyo, M. I.; Perez-Mato, J. M.; Capillas, C.; Kroumova, E.; Ivantchev, S.; Madariaga, G.; Kirov, A.; Wondratschek, H. *Z. Kristallogr.* **2006**, *221*, 15.
(35) Aroyo, M. I.; Kirov, A.; Capillas, C.; Perez-Mato, J. M.; Wondratschek, H. *Acta Crystallogr.* **2006**, *A62*, 115.
(36) Blöchl, P. E.; Jepsen, O.; Andersen, O. K. *Phys. Rev. B* **1994**, *49*, 16223.
(37) Bloss, F. D. *Crystallography and Crystal Chemistry*; Holt, Rinehart, and Winston: New York, 1971.
(38) Decremps, F.; Datchi, F.; Saitta, A. M.; Polian, A.; Pascarelli, S.; DiCicco, A.; Itié, J. P.; Baudelet, F. *Phys. Rev. B* **2003**, *68*, 104101.
(39) Schleife, A.; Fuchs, F.; Furthmüller, J.; Bechstedt, F. *Phys. Rev. B* **2006**, *73*, 245212.
(40) *Handbook of Chemistry and Physics*, 79th ed.; Lide, D. R., Ed.; CRC: Boca Raton, FL, 1998.
(41) Karzel, H.; Potzel, W.; Köfferlein, M.; Schiessl, W.; Steiner, M.; Hiller, U.; Kalvius, G. M.; Mitchell, D. W.; Das, T. P.; Blaha, P.; Schwarz, K.; Pasternak, M. P. *Phys. Rev. B* **1996**, *53*, 11425.
(42) Zhang, J. *Phys. Chem. Miner.* **1999**, *26*, 644.
(43) Liu, H.; Mao, H. K.; Somayazulu, M.; Ding, Y.; Meng, Y.; Häusermann, D. *Phys. Rev. B* **2004**, *70*, 094114.
(44) Ovsyannikova, I. A.; Moroz, E. M.; Platkov, A. I. *Inzh. Fiz. Zh.* **1972**, *22*, 735.
(45) Glans, P. A.; Learmonth, T.; Smith, K. E.; Guo, J.; Walsh, A.; Watson, G. W.; Terzi, F.; Egdell, R. G. *Phys. Rev. B* **2005**, *71*, 235109.
(46) *Relativistic Electronic Structure Theory. Part 2: Applications*; Schwerdtfeger, P., Ed.; Elsevier: Amsterdam, The Netherlands, 2004.
(47) Christensen, N. E.; Seraphin, B. O. *Phys. Rev. B* **1971**, *4*, 3321.
(48) Reizer, M. Yu. *Phys. Rev. B* **1989**, *40*, 11571.
(49) Takeuchi, N.; Chan, C. T.; Ho, K. M. *Phys. Rev. B* **1989**, *40*, 1565.
(50) Elsasser, C.; Takeuchi, N.; Ho, K. M.; Chan, C. T.; Braun, P.; Fahnle, M. *J. Phys.: Condens. Matter* **1990**, *2*, 4371.
(51) Gaston, N.; Opahle, I.; Gäggeler, H. W.; Schwerdtfeger, P. *Angew. Chem., Int. Ed.* **2007**, *46*, 1663.
(52) Söhnel, T.; Hermann, H.; Schwerdtfeger, P. *Angew. Chem., Int. Ed.* **2001**, *40*, 4381.
(53) Söhnel, T.; Hermann, H.; Schwerdtfeger, P. *J. Phys. Chem. B* **2005**, *109*, 526.
(54) Kurzydłowski, D.; Grochala, W. *Chem. Commun.* **2008**, *9*, 1073.
(55) Kurzydłowski, D.; Grochala, W. *Z. Anorg. Allg. Chem.* **2008**, *634*, 1082.
(56) Szentpály, L. v. *J. Phys. Chem. A* **2008**, *112*, 12695.
(57) Desgreniers, S. *Phys. Rev. B* **1998**, *58*, 14102.
(58) Cai, J.; Chen, N. *J. Phys.: Condens. Matter* **2007**, *19*, 266207.
(59) Jaffe, J. E.; Snyder, J. A.; Lin, Z.; Hess, A. C. *Phys. Rev. B* **2000**, *62*, 1660.
(60) Guerrero-Moreno, R. J.; Takeuchi, N. *Phys. Rev. B* **2002**, *66*, 205205.
(61) Singh, V. B. *Indian J. Pure Appl. Phys* **1971**, *9*, 367.
(62) Hanafi, Z. M.; Ismail, F. M. *Z. Phys. Chem.* **1988**, *158*, 81.
(63) Cococcioni, M.; Gironcoli, S. D. *Phys. Rev. B* **2005**, *71*, 035105.
(64) Bouchet, J.; Silberchicot, B.; Jollet, F.; Pasturel, A. *J. Phys.: Condens. Matter* **2000**, *12*, 1723.
(65) Anisimov, V. I.; Zaanen, J.; Andersen, O. K. *Phys. Rev. B* **1991**, *44*, 943.
(66) Moore, C. E. *Atomic Energy Levels*, Natl. Bur. Stand. (U.S.) Circ. No. 467; U.S. GPO: Washington, DC, 1958.

JP9025915